STRAIN ENERGY DENSITY – A MOLECULAR APPRAISAL

D. Y. Tzou* and James C. Dowell

ABSTRACT

The interaction potential between two clusters simulating the crack tip on the lattice level is derived in this work. Employing molecules as the building blocks and the Lennard-Jones potential as the Green's function, the close-form solution shows that the $1/r$-type of singularity is an intrinsic behavior of the energy field when mutual attraction dominates the lattice interactions. This behavior is now proven, explicitly, to be independent of the constitutive equation of the material.

Key Words: molecules, clusters, energy potential, cracks

I. INTRODUCTION

Fracture toughness is a material property that measures the resistance to crack extension in a solid under excessive loading. It results from the abrupt change of the geometrical curvature at the crack tip, giving rise to a singular behavior of stress, strain, and/or strain energy density as the crack tip is sufficiently approached. The continuum theory results in an infinite value of stress, strain, and strain energy density right at the crack tip. In the immediate vicinity of the crack tip, mathematically, the intensity factor results from the finite value of zero (the distance measured from the crack tip) times infinity (the singular field in the near-tip region),

$$F \equiv \lim_{r \to 0} r^n Y(r, \theta; n, a) \tag{1}$$

In Eq. (1), F represents the intensity factor, a is the crack length, (r, θ) is the polar coordinates measuring the location from the crack tip, n is in general a material-dependent exponent, and Y stands for the asymptotic field near the crack tip, which can be stress, strain, or strain energy density function, depending on the way in which the fracture toughness is defined. To make a finite value of F as r approaches zero, obviously, the asymptotic field must possess a singularity of the same order, i.e.,

$$\lim_{r \to 0} Y(r, \theta; n) = \frac{y(\theta; n, a)}{r^n} \tag{2}$$

With the singularity absorbed by r^n, as $r \to 0$, the angular distribution is described by the function $y(\theta; n, a)$. The intensity factor reaches a maximum (minimum) value, termed $y_{\max}(\theta_{\max}; n, a)$ ($y_{\min}(\theta_{\min}; n, a)$), which occurs at a particular angle $\theta_{\max}$ ($\theta_{\min}$) surrounding the crack tip. Combining Eqs. (1) and (2), the intensity factor can thus be expressed as:

$$F = y(\theta; n, a) \equiv \begin{cases} y_{\max}(\theta_{\max}; n, a) \\ y_{\min}(\theta_{\min}; n, a) \end{cases} \tag{3}$$

A macrocrack becomes unstable as the intensity factor F approaches the fracture toughness, which is a material property determined under plan-strain conditions.

Success in the use of the intensity factor in characterizing the stability of a crack is thus predominant by the *prior* knowledge of the singularity of the material response near the crack tip, which depends on the constitutive behavior of the material in general. In linear elastic solids where stress is proportional to strain, for example, it is known that $\sigma_{ij} \sim 1/\sqrt{r}$, or $n = 1/2$ with Y representing generic stress in Eq. (2). The *stress* intensity factor defined in Eq. (3) reduces to the familiar expression $\sigma(\sqrt{(\pi a)})$, with a being the half crack-length. Since stress is proportional to strain in elastic response and strain energy density is proportional to the product between stress and strain, the $1/\sqrt{r}$-singularity in stress and strain results in a $1/r$-singularity in the strain energy density, or $Y \equiv (dW/dV) \sim 1/r$ and $n=1$. The order of singularity, n, varies with

*Corresponding author. (Email: tzour@missouri.edu)

The authors are with the Department of Mechanical and Aerospace Engineering, University of Missouri-Columbia, Columbia, MO 65211, USA.

the quantity (stress or strain energy density) that is used to characterize the crack instability, but is independent of the material property in the elastic response due to the simple relation in stress and strain. The situation becomes more complicated should strain hardening be present in the near-top region (Hutchinson, 1968; Rice and Rosengren, 1968). The near-tip stress singularity strongly depends on the strain-hardening exponent in the stress-strain curve, which needs to be determined beforehand in defining the stress intensity factor around the crack tip. The nonlinear stress-strain relation, though not obvious, still results in a $1/r$-type of singularity in the strain energy density in presence of strain-hardening. In the use of the strain energy density function to characterize the crack instability in a strain hardening materials, in other words, the order of singularity remains identical, n=1.

The standing $1/r$-type of singularity of the strain energy density sheds light on defining the intensity factor that is independent of the constitutive relation of the material. Because of the universal order of singularity, $(dW/dV) \sim 1/r$ or n=1, the resulting intensity factor, termed the strain energy density factor (Sih, 1973), possesses a unique feature that a *prior* knowledge of the stress singularity in the near-tip region is not required. Such an invariant behavior in the near-tip region, most importantly, facilitates a universal definition of the fracture toughness for characterizing the crack instability in both linear and nonlinear materials. The resulting approach is termed the strain energy density theory, or the S-theory after George C. Sih.

While the S-theory has been universally examined and applied to a wide variety of materials with cracks, a fundamental question remains: What is the fundamental structure, in solids, that result in the universal $1/r$-behavior near the crack tip? As the stress-strain relation varies, a painful approach would be performing the stress analysis in accordance and prove that the resulting strain energy density does vary with $1/r$. The HRR solutions in strain hardening materials are examples. The advantage of this approach is to derive the stress (strain) singularity as a byproduct. The disadvantage, however, lies in that the resulting $1/r$-behavior is from the presumed stress-strain relation. In view of the capricious constitutive behavior of materials, most detrimentally, this approach is non-conclusive by nature. There exists an argument that Newton's law of gravitation results in a 1/r behavior for celestial bodies in attraction. The way in which the celestial bodies in cosmological scale resemble the lattice structure in small scale, however, remains blurred.

The present work revisits the strain energy density function, aiming at investigating the $1/r$-behavior around the crack tip from a molecular point of view. The Lennard-Jones (LJ) potential is used to describe the intermolecular interactions. The LJ potential is then used as the Green's function to establish the cluster potential as the molecules congregate. As the distance between two molecular clusters becomes close, just like the lattice structure in the vicinity of a crack tip, it is shown that the intermolecular attraction indeed behaves as $1/r$, with r being the distance measured from the crack tip. Since the molecular approach is in the atomistic scale, it does not employ any constitutive equation that only applies in the continuum scale. The resulting $1/r$-behavior, therefore, is an intrinsic behavior of the strain energy density function that is independent of the constitutive relation.

II. CLUSTER POTENTIAL

In approaching a crack tip sufficiently close, eventually, we expect to see a number of molecules interacting with each other, with the crack tip characterized by a few molecules under imposed geometrical constraints. This is the basis that molecular dynamics (MD) simulation has been active in recent years that aims to study the crack instability from a molecular point of view. Such simulation on the molecular level, obviously, eliminates all the empirically based relations, including the constitutive equation, where an unstable crack results directly from the separation of molecules near the crack tip. The classical MD simulation employs Newton's law of motion to describe two interacting molecules, say i and j,

$$m_i \ddot{x}_i = \sum_{\substack{j=1 \\ j \neq i}}^{N} F_{ij} = \sum_{\substack{j=1 \\ j \neq i}}^{N} - \nabla U(x_i, x_j) ;$$

$$m_j \ddot{x}_j = - \sum_{\substack{j=1 \\ j \neq i}}^{N} F_{ij} = \sum_{\substack{k=1 \\ k \neq i}}^{N} \nabla U(x_i, x_j) \qquad (4)$$

where the subscripts refer to the molecules, m is the molecular mass, F_{jk} is the interaction force between molecules j and k, $U(x_j, x_k)$ is the intermolecular potential between molecules j and k at x_j and x_k, respectively, ∇U stands for the gradient of U, and N the number of molecules in the molecular assembly. The negative sign in the second expression of Eq. (4) results from Newton's third law of motion. Subjecting to a specified intermolecular potential, Eq. (4) requires the solutions of $3N$ nonlinearly coupled ordinary equations for x_i and $\dot{x}_i$. While a physical event, such as the crack instability and material ablation (Tzou *et al*., 2004), can be observed directly from the dynamic (time-dependent) evolution of the molecular separation, the molecular displacement and velocity are essential quantities to calculate the

thermomechanical properties (such as elastic moduli and thermal conductivity) of the material without attributing to any constitutive relation. The MD simulation, in essence, derives the constitutive relation that sensitively varies with the local environment such as temperature and strain rate.

1. Lennard-Jones (LJ) Potential

Crack surfaces, from a microscopic point view as shown in Fig. 1(a), are composed of a special group of molecules under constrained motion. Interacting with other molecules in the physical domain around the crack tip, in a quasi-stationary or equilibrium state, such specially constrained molecules oscillate around their time-averaged locations that define a crack surface on a larger physical scale. The amplitude of the molecular oscillations is much smaller than the time-averaged profile of the crack surface, making the crack surface, including its tip, appears stationary. Meanwhile, all other molecules interacting with this special group of molecules also oscillate around their equilibrium positions. The time-averaged (stationary) configurations of these molecules define the equilibrium state near the crack tip. Crack instability results from displacement of the molecules from their equilibrium positions, either by externally applied load or laser energy. As a result, the molecules defining the crack surface (tip) may undergo another dynamic evolution and the crack may become unstable should the interactions with other molecules nearby result in a new equilibrium state (metastable or stable crack growth) or a permanent separation (catastrophic crack propagation). Crack instability can certainly be investigated by keeping track of the individual behaviors of all attending molecules in the near-tip region. The limitation of the computational power, which allows for a simultaneous treatment of about 10^8 molecules (comparing to 10^{23} molecules for one mole) for the time being, however, seriously restricts the resolution that is sufficient for a conclusive result. Observing the natural tendency of molecular agglomeration when interacting with each other, in a similar concept to the lattices on mesoscale, an alternate approach is to group the interacting molecules in the various clusters, as shown in Fig. 1(a). Instead of the individual behaviors of molecules, this approach describes the group behavior of clusters in studying the mechanical behavior near the crack tip.

The intermolecular potential, $U(x_i, x_j)$ with $r_{ij}=|x_i-x_j|$ representing the distance between molecule i and molecule j, as shown in Fig. 1(b), dominates the molecular motion described by Eq. (4). The

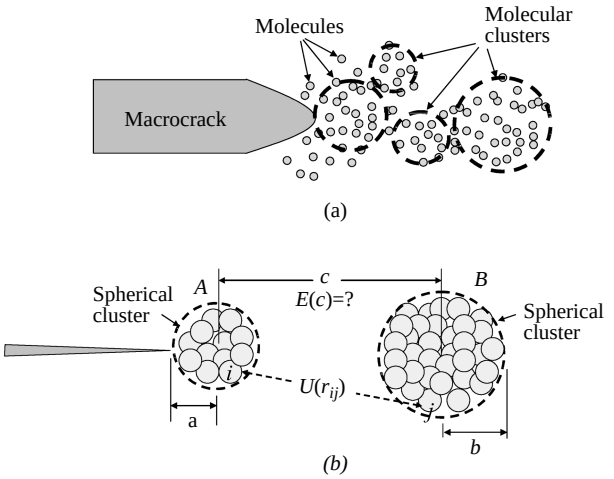

Fig. 1. (a) Molecular clusters (lattices) in the immediate vicinity of a crack tip. (b) Molecules contained in each cluster and the cluster potential $E(d)$, where d is the central distance between two adjacent clusters.

Lennard-Jones potential (ICHMT Symposium, 1996; Chou *et al*., 1999),

$$U_{ij} \equiv U(x_i, x_j) = \frac{C_1}{r_{ij}^{12}} - \frac{C_2}{r_{ij}^{6}}$$

$$F_{ij} = -\frac{dU_{ij}}{dr_{ij}} = \frac{12C_1}{r_{ij}^{13}} - \frac{6C_2}{r_{ij}^{7}} \tag{5}$$

which is a special type of the Van der Walls force, may be the most representative due to its simple form and well tabulated model parameters for real substances. For argon gas, for example, C_1=1.61164 $\times 10^{-134}$ (J-m^{12}) and C_2=1.03229$\times 10^{-77}$ (J-m^6). They are also the threshold values for LJ solids in general due to the nature of the Van der Walls force formulated on the molecular level.[1] The first term on the right-hand-side of Eq. (5) represents the repulsive potential ($\sim 1/r_{ij}^{12}$) as two molecules become very close. The second term, which always bears a negative sign, represents the attractive potential ($\sim 1/r_{ij}^{6}$). The equilibrium position between two molecules, denoted by r_0, separates the repulsive and attractive regimes and is dictated by

$$F_{ij}(r_0)=0 \Rightarrow r_0 = \left(\frac{2C_1}{C_2}\right)^{1/6} \tag{6}$$

The equilibrium position (r_0) is of the order of 10^{-1} nm for most real substances. Using the typical values of $C_1=10^{-26}$ (J-nm^{12}) and $C_2=10^{-23}$ (J-nm^6), r_0= 0.35 nm.

[1] For copper, Tzou *et al*. (2004), for example, C_1=1.81656$\times 10^{-135}$ (J-m^{12}) and C_2=1.60219$\times 10^{-77}$ (J-m^6), as compared to the EMA (embedded atomic method)potential. For silicon, C_1=2.17571$\times 10^{-132}$ (J-m^{12}) and C_2=9.90068$\times 10^{-76}$ (J-m^6) as compared to the Morse potential.

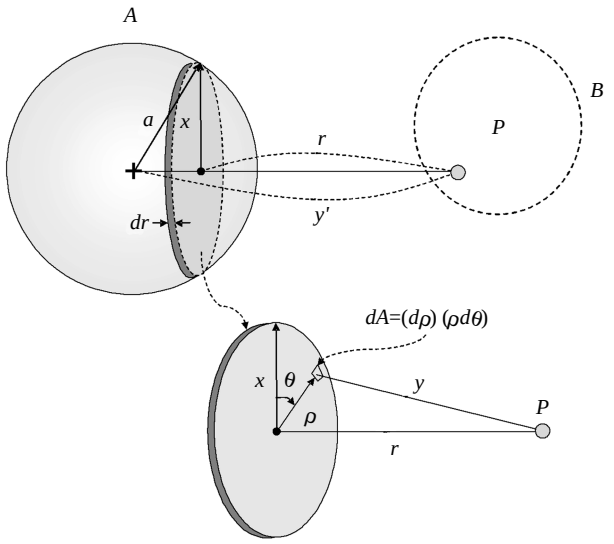

Fig. 2. Potential between a representative molecule P in sphere B and sphere A – The Coordinate system.

Note that in applying Eq. (4) to describe the molecular motion, a stationary configuration for the attending molecules is impossible even in a steady state. Due to the acceleration term that displays a wave behavior by nature, the so-called equilibrium position is the time-averaged position, around which the two molecules oscillate. A harmonic oscillator could be imagined as a qualitative behavior in the MD simulation, regardless of the number of molecules that are used in modeling the physical response.

2. Molecular Clustering

Clustering of molecules is a natural tendency in the preparation of nanomaterials (Siegel, 1996). In modeling the mesoscale response near a crack tip, the concept of molecular clusters is particularly useful because it closely resembles the lattices that are typically on the order of 0.1 - 1 μm. This concept is illustrated in Fig. 1(a), where interactions among molecular clusters (lattices) dominate over the individual behaviors of molecules – particularly in making contact with the continuum behavior on a larger physical scale. One lattice, which is now viewed as a molecular cluster, contains several hundreds to a few thousands molecules. These molecules may still move within one cluster as a result of the mutual interactions, but the magnitude is much smaller than the relative motion among clusters. Such molecules thus "congregate" in one cluster, as sketched in two spheres in Fig. 1(b). They move with the cluster as a group, and the group behavior of such clusters is a key to bridge together the physical behaviors on the molecular and continuum levels.

The LJ potential prevails for each pair of molecules in adjacent clusters, as shown by molecule *i* (in cluster A) and molecule *j* (cluster B) in Fig. 1(b). The two clusters, assumed spherical in shape with radii being *a* and *b*, respectively, are representative lattices near the crack tip in Fig. 1(a). To determine the cluster potential, $E(d)$ in Fig. 1(b) with *d* representing the distance between the centers of spheres A and B, let us assume numerous but uniformly distributed molecules in each sphere. The volumetric number densities of molecules in each sphere is represented by m_A (in sphere A) and m_B (sphere B), respectively.

First consider the interaction potential between a representative molecule (P) in sphere B with the spherical cluster A. The distance between the molecule P and center of sphere A is denoted by y', and the distance between P and a representative disk of radius *x* in sphere A is denoted by *r*. The LJ potential exerts on P and $dA=\rho d\rho d\theta$, which is an infinitesimal area on the representative disk. Replacing r_{ij} in Eq. (5) by $y=(\rho^2+r^2)^{1/2}$ and representing the LJ resulting potential by $U(y)$, the two-dimensional interaction potential, $E_{M\text{-}D}(x, r)$, between P and the disk results from integrating $U(y)$ over the entire disk of radius *x*:

$$E_{M-D}(x,r) = m_{A\rho}\int_0^x U(y)\Big|_{y=\sqrt{\rho^2+r^2}} \cdot \rho d\rho \int_0^{2\pi} d\theta$$

$$= 2\pi m_{A\rho}\{C_1[\frac{1}{10r^{10}} - \frac{1}{10(r^2+x^2)^5}]$$

$$- C_2[\frac{1}{4r^4} - \frac{1}{4(r^2+x^2)^2}]\} \qquad (7)$$

where $m_{A\rho}$ measures the number of molecules per unit area on the disk. In the case that P is very close to the disk, $r<<x$, Eq. (7) reduces to

$$E_{M-D}(r) = 2\pi m_{A\rho}(\frac{C_1}{10r^{10}} - \frac{C_2}{4r^4}) \quad \text{for} \quad r<<x \qquad (8)$$

The repulsive and attractive indices in the molecule-to-disk potential ($E_{M\text{-}D}$) sensitively change from the 12-6 relation (LJ) to the 10-4 relation. Smaller values of the attractive and repulsive indices in the cluster potential imply a shorter equilibrium distance and a shallower potential-well depth than the L-J potential. This is due to the larger mass of clusters as molecules congregate into a certain shape, forming a heavier body that pulls the surrounding molecules closer in approaching mechanical equilibrium.

The molecule-to-disk potential can now be integrated to obtain the molecule-to-sphere potential.

This is done by integrating $E_{M\text{-}D}$ in Eq. (7) over the entire sphere A, with r ranging from $(y'-a)$ to $(y'+a)$. The interaction potential between molecule P and sphere A of a distance y' apart is thus

$$E_{M-S}(y') = \int_{y'-a}^{y'+a} E_{M-D}(x,r)\big|_{x=\sqrt{a^2-(y'-r)^2}} \cdot m_{Ar}\,dr$$

$$= 2\pi m_A\{-\frac{C_1}{10}[\frac{1}{9(y'+a)^9}-\frac{1}{9(y'-a)^9} - \frac{1}{8y'(y'+a)^8}+\frac{1}{8y'(y'-a)^8}] + \frac{C_2}{4}[\frac{1}{3(y'+a)^3}-\frac{1}{3(y'-a)^3}-\frac{1}{2y'(y'+a)^2} + \frac{1}{2y'(y'-a)^2}]\} \qquad (9)$$

where m_A ($=m_{Ar}\times m_{A\rho}$) is the number density of molecules per unit volume in sphere A. For the case that the molecule is very close to the spherical cluster, i.e., $d<<a$ with $d(=y'-a)$ being the distance between P and the *surface* of sphere A, the near-field potential parallel to Eq. (8) is

$$E_{M-S} = \pi m_A(\frac{C_1}{45d^9}-\frac{C_2}{6d^3}) \quad \text{for} \quad d<<a \qquad (10)$$

The 10–4 relation ($E_{M\text{-}D}$) further evolves into a 9–3 relation ($E_{M\text{-}S}$). As the dimensionality of the cluster increases by one, from a disk (2D) to a sphere (3D), for example, the exponent characterizing the attractive (repulsive) potential decreases by one. The difference between the repulsive and attractive exponents, however, remains at six (6) all the time.

The molecule-to-sphere potential, $E_{M\text{-}S}(y')$ in Eq. (9), can now be used as the basic potential between sphere A and a differential area dA' ($=d\rho'\times \rho'\,d\theta'$) that is located on a representative disk in sphere B, as shown in Fig. 3, with $y'=\sqrt{\rho'^2+R^2}$ being the distance between the center of sphere A and dA'. The sphere-to-disk potential, $E_{S\text{-}D}(x', R)$, then results from the surface integration over the disk in sphere B, with $0\le\rho'\le x'$ and $0\le\theta'\le 2\pi$:

$$E_{S-D}(x',R) = m_{B\rho}\int_0^{x'} E_{M-S}(y')\big|_{y'=\sqrt{\rho'^2+R^2}} \cdot \rho' d\rho' \int_0^{2\pi} d\theta' \qquad (11)$$

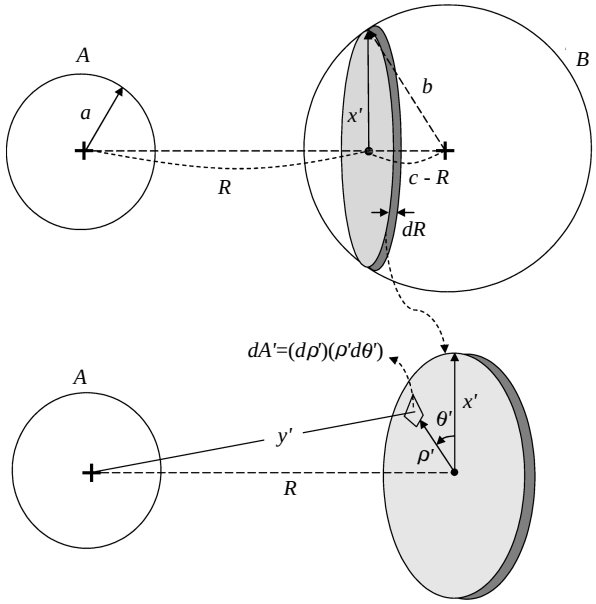

Fig. 3. Representative disk of differential thickness dR in spherical cluster B and the planar coordinate system.

where $m_{B\rho}$ is the number of molecules per unit area on the disk and R is the distance between the center of sphere A and the representative disk in sphere B. The sphere-to-sphere potential, $E_{S\text{-}S}$, finally, results from the integration of $E_{S\text{-}D}$, in sphere B, from $R=(c-b)$ to $(c+b)$ with $x'=\sqrt{b^2-(c-R)^2}$ and c the central distance between spheres A and B:

$$E_{S-S}(c;a,b) = m_{BR}\int_{c-b}^{c+b} E_{S-D}(x',R)\big|_{x'=\sqrt{b^2-(c-R)^2}} \cdot dR$$

$$= \pi^2 m_A m_B\{\frac{C_1}{37800c}[\frac{c^2+7gc+G}{(c+g)^7}+\frac{c^2-7gc+G}{(c-g)^7} - \frac{c^2+7hc+H}{(c+h)^7}-\frac{c^2-7hc+H}{(c-h)^7}] - \frac{C_2}{6}[\frac{2ab}{c^2-g^2}+\frac{2ab}{c^2-h^2}+\ln\frac{c^2-g^2}{c^2-h^2}]\} \qquad (12)$$

where, in parallel to that in Eq. (9), $m_B=m_{B\rho}\times m_{BR}$, $g=a+b$, $h=a-b$, $G=6a^2+6b^2+42ab$, and $H=6a^2+6b^2-42ab$. The sphere-to-sphere potential is thus a function of c, the central distance between spheres A and B, with a (radius of sphere A) and b (radius of sphere B) appearing as two parameters. The interaction force between two spheres is simply the gradient of $E_{S\text{-}S}$, $F=-dE_{S\text{-}S}/dc$, where c is equivalent to the distance between two molecules, r_{ij} in Eq. (5).

Cluster interaction between two identical spheres poses a close approximation in engineering materials. In this case, $b=a$ and $m_A=m_B=m$, and Eq. (12) reduces to

$$E_{S-S} = \pi^2 m^2 \{\frac{C_1}{37800c}[\frac{c^2+54a^2+14ac}{(c+2a)^7} + \frac{c^2+54a^2-14ac}{(c-2a)^7} + \frac{2c^2-60a^2}{c^7}] - \frac{C_2}{6}[\frac{2a^2}{c^2-4a^2} + \frac{2a^2}{c^2} + \ln\frac{c^2-4a^2}{c^2}]\}$$

(identical spherical clusters) (13)

Consequently,

$$F_{S-S} = -\frac{dE_{S-S}}{dc} = \pi^2 m^2 \{\frac{C_1}{37800c^2}[\frac{6c^3+96ac^2+432a^2c+108a^3}{(c+2a)^8} + \frac{6c^3-96ac^2+432a^2c-108a^3}{(c-2a)^8} - \frac{12c^2-480a^2}{c^7}] - \frac{C_2}{3}[\frac{2a^2c}{(c^2-4a^2)^2} + \frac{2a^2}{c^3} - \frac{c}{c^2-4a^2} + \frac{1}{c}]\}$$

(identical spherical clusters) (14)

III. ASYMPTOTIC FORM

On the mesoscale surrounding the crack tip, without an additional defect, the lattices are very close to each other. In terms of the distance between the surfaces of two spheres shown in Fig. 1, $d=c-(a+b)$, the condition for lattices with integrity implies $d<<a$ and $d<<b$. Replacing c by $d+(a+b)$ in Eq. (12) and applying the Taylor series expansion to the result,

$$E_{S-S} \cong \frac{\pi^2 m_A m_B ab}{a+b}\{\frac{C_1}{1260d^7} - \frac{C_2}{6d}\}$$

for $d<<a$, $d<<b$ (15)

The 9-3 relation of the molecule-to-sphere potential ($E_{M\text{-}S}$) finally evolves into a 7-1 relation for the sphere-to-sphere potential ($E_{S\text{-}S}$). The repulsive potential is represented by the $1/d^7$-term, which is unlikely for two lattices (clusters) interacting on mesoscale. The potential energy for attraction, represented by the second $1/d$-term in Eq. (15), hence reflects the deformation energy as two clusters are displaced in the near-tip region. The resulting energy potential is

$$E_{S-S} \cong -\frac{\pi^2 m_A m_B ab}{a+b}(\frac{C_2}{6d}) \text{ for } d<<a,\ d<<b \quad (16)$$

In case of identical clusters with equal radius, $b=a$ and $m_A=m_B=m$, Eq. (15) reduces to

$$E_{S-S} = \pi^2 m^2 a\{\frac{C_1}{2520d^7} - \frac{C_2}{12d}\} \text{ for } d<<a \quad (17)$$

whose attractive component, in correspondence with Eq. (16), is

$$E_{S-S} = -\pi^2 m^2 a(\frac{C_2}{12d}) \text{ for } d<<a \quad (18)$$

From either Eq. (16) or (18), it is evident that as two spherical clusters are sufficiently close, $d<<a$, the potential energy between them is inversely proportional to the surface distance d, i.e., $E\sim 1/d$. As a meso/macroscale crack tip is approached sufficiently close, therefore, clusters (lattices) will take over the mechanical interactions and the $1/d$-behavior derived in Eq. (16) or (18) resembles the $1/r$-singularity preserved in the strain energy density function near the crack tip. In parallel to the volumetric (surface) energy-density concept, divide $E_{S\text{-}S}$ by the volume (surface) of the spherical cluster of radius a to yield

$$\frac{E_{S-S}}{(4\pi a^3/3)} = -(\frac{\pi m^2 C_2}{16a^2})\frac{1}{d} \sim \frac{1}{d};$$

$$\frac{E_{S-S}}{(4\pi a^2)} = -(\frac{\pi m^2 C_2}{48a})\frac{1}{d} \quad (19)$$

In case of moving clusters, kinetic energy needs to be included in addition to inter-sphere potential (E). The negative sign results from the way attraction is distinguished from repulsion on the molecular level, see Eq. (5).

The interaction force between two spheres can be found from Eqs. (16) and (18),

$$F_{S-S} = -\frac{\mathrm{d}E_{S-S}}{\mathrm{d}d} = \begin{cases} \frac{\pi^2 m^2 ab}{a+b}\{\frac{C_1}{180d^8} - \frac{C_2}{6d^2}\} & \text{(different spheres)} \\ \pi^2 m^2 a\{\frac{C_1}{360d^8} - \frac{C_2}{12d^2}\} & \text{(identical spheres)} \end{cases} \quad (20)$$

Such interaction force vanishes at the position

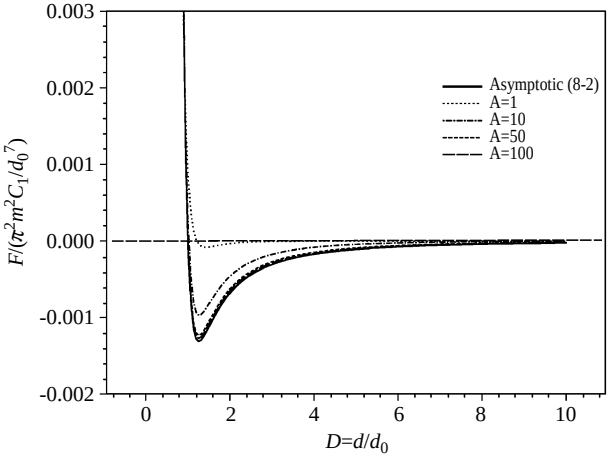

Fig. 4. Comparison of the interaction forces – The asymptotic expression, Eq. (20) with identical spheres (the 8-2 relation), and the full expression, Eq. (14), $A=a/d_0$.

of equilibrium, $F_{S\text{-}S}(d_0)=0$, resulting in $d_0=[C_1/(30C_2)]^{1/6}$. The equilibrium position is independent of the size (a or b) of the spherical cluster. For copper with a FCC crystal structure, $d_0 \sim 1.22$Å, as compared to its atomic radius 1.3Å. Repulsive force prevails in the physical domain of $d<d_0$ whereas attractive force dominates in $d>d_0$. As many copper atoms agglomerate in one cluster, obviously, the cluster size (radius a) is much larger than d_0 and the attractive potential ($E \sim 1/d$) indeed dominates the interactions among clusters.

Interaction forces depend on the radius (a) of the spherical cluster, referring to the full expression shown by Eq. (14). For cluster interactions involving identical spheres, Fig. 4 compares Eq. (14) (the full expression) with the second expression in Eq. (20) (the asymptotic, 8-2 relation) at different values of the radius. Both the radius (a) and the surface distance (d) are normalized with respect to the equilibrium distance d_0, $A=a/d_0$ and $D=d/d_0$, and the interaction force is normalize with respect to $(\pi^2 m^2 C_1/d_0^7)$. The force reduces to zero at the equilibrium position, $D=1$ or $d=d_0$. The magnitude of the attraction force (in the domain of $D>1$) increases as the radius of the spherical cluster increases. The asymptotic (8-2) relation becomes a close approximation as A exceeds 50, or $a>50d_0$. The interaction force vanishes for $D>8$ or $d>8d_0$. This is the cutoff radius in cluster dynamic simulation, beyond which the force terms in Eq. (4) can be assumed zero to save computational time with acceptable accuracy. Such a cutoff radius is greater than that in molecular dynamic simulation ($d>2.6d_0$), because the cluster carries a heavier mass and consequently the range of influence is longer.

In passing, note that the results derived so far are not restricted by the geometry of the clusters. The 7-1 relation, and hence the $1/d$-behavior, as two clusters become close applies in general to clusters of any shape. The only difference lies in the shape factors, which need to be calculated numerically, in place of the simple parameters such as 6, 180, a and b in Eq. (20) resulting from spherical clusters.

IV. CONCLUSION

The interaction potential among clusters, which simulate the deformation lattices in the physical domain close to a crack tip, has been derived analytically. The close-form solution is intended to precisely derive the $1/r$-behavior of the strain energy density function in the S-theory of fracture mechanics, with r now being replaced by the surface distance between two interacting spheres - One is exactly at the crack tip and another is in the neighborhood of the crack tip. The $1/r$-behavior of the energy density, now appears to be intrinsic, nicely extends the mechanical behavior from the continuum level to the lattice level, as long as the molecules distribute uniformly in the lattice. Extension of the S-theory, including the trans-scale iso-energy density concept that Sih (2001) has developed over the past two decades, is thus natural in the continuous reduction of the physical scale. This result should not be surprising, however, because energy, unlike stress, is indeed a physical quantity that exists in any physical scale. Its wider coverage in interpreting the physical response crossing several physical scales is expected.

There is no continuum theory that supports calculation of the strain energy (density) without going through the stress analysis. The $1/r$-behavior of the strain energy density in the near-tip region, unavoidably, has been viewed as an aftermath of the stress analysis that strongly depends on the constitutive equation. The close-form solutions for the interaction potential derived in this work, on the other hand, shows that the $1/r$-behavior is preserved all the way to the molecular level, which is independent of the constitution of the material. The clusters described in this work are uniform assemblies of molecules, which resemble the lattice structure in engineering materials.

The cluster potential has been extended to simulate the superheated melting and ultrafast ablation in metals and semiconductors subjected to petawatts, femtosecond laser irradiation (Chen *et al.*, 2004, Tzou *et al.*, 2004). The excessively high strain rate and heating rate in this type of problem make it extremely difficult to model the continuum response due to the unknown constitutive relations. The cluster dynamic simulation not only provides fine resolutions for the onset and evolution of such ultrafast failure, it also

allows for interactions among clusters and molecules in sensitive areas where a finer resolution is further demanded. The 9-3 relation derived in Eq. (10) for molecule-to-sphere interactions replaces the 7-1 relation for sphere-to-sphere interactions as molecules are instated in the computational domain. The interaction potential between a spherical cluster and a flat surface modeling a physical boundary, most attractively, is a limiting case of $b\to\infty$ in Eq. (12). Consequently, the 7-1 relation shown by Eq. (17) remains, with the coefficients 2520 and 12 replaced by 1260 and 6, respectively. Cluster interactions with a physical boundary can thus be modeled by a simple change of the coefficients without the use of the artificially imposed computational cells with symmetry. From the examples of cluster-to-molecule and cluster-to-plane interactions that may cover several orders of magnitude in physical scales, it is evident that the cluster dynamic simulation offers a unique approach in modeling physical systems with true multiscale interactions.

NOMENCLATURE

a	radius of the cluster or crack length, m
A	nondimensional radius relative to the equilibrium distance
A	sphere A
B	sphere B
b	radius of the cluster, m
c	distance between centers of two clusters, m
C_1	repulsive coefficient in the Lennard-Jones potential, J m^{12}
C_2	attractive coefficient in the Lennard-Jones potential, J m^6
d	distance between surfaces of two clusters, m
D	nondimensional surface distance relative to the equilibrium distance
E	potential energy, J
F	intermolecular force, N, or intensity factor
ij	molecule i and j
m	volumetric density of molecules, $1/m^3$
M-D	molecule to disk
n	power of singularity
r	distance, m
R	distance, m
S-D	sphere to disk
S-S	sphere to sphere
U	Lennard-Jones potential, J
x	disk radius, m
$\dot{x}$	dx/dt, time-derivative of x
y	distance, m
y'	distance, m
Y	angular distribution
θ	polar angle, radiant
ρ	distance, m
0	equilibrium state

REFERENCES

Chen, J. K., Beraun, J. E., Roybal, R., and Tzou, D. Y., 2004, "Nano- to Microscale Modeling by Cluster Potentials," *AIAA Journal of Thermophysics and Heat Transfer*, Vol. 18, No. 2, pp. 253-262.

Chou, F. C., Lukes, J. R., Liang, X.-G., Takahashi, K., and Tien, C. L., 1999, "Molecular Dynamics in Microscale Thermophysical Engineering," *Annual Review of Heat Transfer*, Vol. X, C. L. Tien ed., Begell House, New York, USA, pp. 141-176.

Hutchinson, J. W., 1968, "Plastic Stress and Steain Fields at a Crack Tip," *Journal of the Mechanics and Physics of Solids*, Vol. 16, pp. 337-347.

ICHMT Symposium on Molecular and Microscale Heat Transfer in Materials Processing and Other Applications, 1996, Vols. 1 and 2, Yokohama, Japan.

Rice, J. R., and Rosengren, G. F., 1968, "Plane Strain Deformation Near a Crack Tip in a Power Law Hardening Material," *Journal of the Mechanics and Physics of Solids*, Vol. 16, pp. 1-12.

Siegel, R. W., 1996, "Creating Nanophase Materials," *Scientific American*, pp. 74-79.

Sih, G. C., 1973, *Methods of Analysis and Solutions of Crack Problems, Mechanics of Fracture*, Vol. 1, Noordhoff, Leyden, The Netherlands.

Sih, G. C., 2001, "Implication of Scaling Hierarchy Associated with Nonequilibrium: Field and Particulate," *Journal of Theoretical and Applied Fracture Mechanics*, Vol. 37, Nos. 1-3, pp. 335-369.

Tzou, D. Y., Chen, J. K., R. Roybal, and Beraun, J. E., 2004 "Cluster Dynamics Simulation for Multiscale Interactions" *International Journal of Heat and Mass Transfer*, Vol. 47, Nos. 14-16, pp. 2949-2959.

Manuscript Received: Jun. 07, 2004
and Accepted: Jul. 02, 2004